J|A|C|S
ARTICLES
Published on Web 02/05/2008

# $[Re(\eta^5\text{-}C_5H_5)(CO)_3]^+$ Family of 17-Electron Compounds: Monomer/Dimer Equilibria and Other Reactions

Daesung Chong,[†] Derek R. Laws,[†] Ayman Nafady,[†,||] Paulo Jorge Costa,[‡] Arnold L. Rheingold,[§] Maria José Calhorda,[‡] and William E. Geiger*[,†]

*Department of Chemistry, University of Vermont, Burlington, Vermont 05405, Departamento de Química e Bioquímica, Faculdade de Ciências, Universidade de Lisboa, 1749-016, Lisboa, Portugal, and Department of Chemistry and Biochemistry, University of California at San Diego, La Jolla, California 92093*

Received November 29, 2007; E-mail: william.geiger@uvm.edu

***Abstract:*** The anodic electrochemical oxidations of $ReCp(CO)_3$ (**1**, Cp = $\eta^5$-$C_5H_5$), $Re(\eta^5\text{-}C_5H_4NH_2)(CO)_3$ (**2**), and $ReCp^*(CO)_3$ (**3**, Cp* = $\eta^5$-$C_5Me_5$), have been studied in $CH_2Cl_2$ containing $[NBu_4][TFAB]$ (TFAB = $[B(C_6F_5)_4]^-$) as supporting electrolyte. One-electron oxidations were observed with $E_{1/2}$ = 1.16, 0.79, and 0.91 V vs ferrocene for **1**−**3**, respectively. In each case, rapid dimerization of the radical cation gave the dimer dication, $[Re_2Cp^\gamma_2(CO)_6]^{2+}$ (where $Cp^\gamma$ represents a generic cyclopentadienyl ligand), which may be itself reduced cathodically back to the original 18-electron neutral complex $ReCp^\gamma(CO)_3$. DFT calculations show that the SOMO of $\mathbf{1}^+$ is highly Re-based and hybridized to point away from the metal, thereby facilitating the dimerization process and other reactions of the Re(II) center. The dimers, isolated in all three cases, have long metal−metal bonds that are unsupported by bridging ligands, the bond lengths being calculated as 3.229 Å for $[Re_2Cp_2(CO)_6]^{2+}$ ($\mathbf{1_2}^{2+}$) and measured as 3.1097 Å for $[Re_2(C_5H_4NH_2)_2(CO)_6]^{2+}$ ($\mathbf{2_2}^{2+}$) by X-ray crystallography on $[Re_2(C_5H_4NH_2)_2(CO)_6][TFAB]_2$. The monomer/dimer equilibrium constants are between $K_{dim} = 10^5$ $M^{-1}$ and $10^7$ $M^{-1}$ for these systems, so that partial dissociation of the dimers gives a modest amount of the corresponding monomer that is free to undergo radical cation reactions. The radical $\mathbf{1}^+$ slowly abstracts a chlorine atom from dichloromethane to give the 18-electron complex $[ReCp(CO)_3Cl]^+$ as a side product. The radical cation $\mathbf{1}^+$ acts as a powerful one-electron oxidant capable of effectively driving outer-sphere electron-transfer reactions with reagents having potentials of up to 0.9 V vs ferrocene.

## 1. Introduction

The prototypical third-row piano stool complex $ReCp(CO)_3$, **1** (Cp = $\eta^5$-$C_5H_5$), continues to draw new interest in diverse areas, including pharmacological applications.[1] Although its thermal[2] and photolytic[3,4] reactions have been well studied, the anodic electrochemical properties of **1** and its close analogues are essentially unexplored. Hershberger et al. reported briefly that the oxidation of $ReCp(CO)_2L$, L = pyridine or $PPh_3$, is irreversible by voltammetry,[5] but there appears to have been no report on the oxidation of the parent compound **1**. We became interested in exploring the putative 17-electron radical cation $\mathbf{1}^+$. Given the well-known ability of rhenium to adopt seven coordination,[2] it was thought that $\mathbf{1}^+$ might have a potent Re(II) reaction center, unencumbered by steric effects owing to the presence of the three carbonyl ligands.

The isoelectronic *neutral* second- and third-row group 6 forerunners of $\mathbf{1}^+$, namely $MCp(CO)_3$, M = Mo, W, have a rich and well-explored chemistry that is heavily influenced by metal-based radical reactions, including metal−metal dimerizations.[6] Group 7 cationic analogues of these radicals were expected to encounter two issues that might compromise their generation and long-term stability. The fact that significantly more positive potentials[5] would be necessary to oxidize the Re(I) compound suggested that the Re(II) product would be quite electrophilic, raising the likelihood of its encountering nucleophilic attack[7] by a traditional supporting electrolyte anion such as $[PF_6]^-$ or $[BF_4]^-$. An additional difficulty, more methodological in nature, is that, unless there are ligand substituents

[†] University of Vermont.
[‡] Universidade de Lisboa.
[§] University of California at San Diego.
[||] Permanent Address: Chemistry Department, Faculty of Science, Sohag University, Sohag, Egypt 82524.

(1) (a) Cesati,R. R., III; Tamagnan, G.; Baldwin, R. M.; Zoghbi, S. S.; Innis, R. B.; Kula, N. S.; Baldessarini, R. J.; Katzenellenbogen, J. A. *Bioconjugate Chem.* **2002**, *13*, 29.(b) Mull, E. S.; Sattigeri, V. J.; Rodriguez, A. L.; Katzenellenbogen, J. A. *Bioorg. Med. Chem.* **2002**, *10*, 1381.
(2) (a) Caulton, K. G. *Coord. Chem. Rev.* **1981**, *38*, 1. (b) O'Connor, J. M. In *Comprehensive Organometallic Chemistry II*; Abel, E. W., Stone, F. G. A., Wilkinson, G., Eds.; Pergamon Press: Oxford, 1994, Volume 6; pp 210 ff. (c) Boag, N. M.; Kaesz, H. D. In *Comprehensive Organometallic Chemistry*; Wilkinson, G., Stone, F. G. A., Abel, E. W., Eds.; Pergamon Press: Oxford, 1982; Vol. 4, pp 205 ff.
(3) (a) Bergman, R. G.; Cundari, T. R.; Gillespie, A. M.; Gunnoe, T. B.; Harman, W. D.; Klinckman, T. R.; Temple, M. D.; White, D. P. *Organometallics* **2003**, *22*, 2331. (b) Yang, H.; Asplund, M. C.; Kotz, K. T.; Wilkens, M. J.; Frei, H.; Harris, C. B. *J. Am. Chem. Soc.* **1998**, *120*, 10154.
(4) (a) Lawes, D. J.; Darwish, T. A.; Clark, T.; Harper, J. B.; Ball, G. E. *Angew. Chem., Int. Ed.* **2006**, *45*, 4486. (b) Lawes, D. J.; Geftakis, S.; Ball, G. E. *J. Am. Chem. Soc.* **2005**, *127*, 4134. (c) Childs, G. I.; Grills, D. C.; Nikiforov, S. M.; Poliakoff, M.; George, M. W. *Pure Appl. Chem.* **2001**, *73*, 443. (d) Geftakis, S.; Ball, G. E. *J. Am. Chem. Soc.* **1999**, *121*, 6336.
(5) Hershberger, J. W.; Amatore, C.; Kochi, J. K. *J. Organomet. Chem.* **1983**, *250*, 345.


**10.1021/ja710513n CCC: $40.75** 

that enhance their solubilities in low polarity solvents,[6y] dileptic[8] metal carbonyl cations tend to be poorly soluble as salts of the traditional anions in otherwise attractive low-donor solvents such as dichloromethane, adding difficulty to the voltammetric analysis of the oxidation processes.[9,10c] Both of these potential problems are likely to be circumvented by the use of weakly coordinating electrolyte anions (WCEAs).[7c, 9−11] Taking advantage of this medium modification, we now describe the one-electron oxidation of **1** and two of its derivatives, namely the aminocyclopentadienyl complex $Re(C_5H_4NH_2)(CO)_3$, **2**, and the pentamethylcyclopentadienyl complex $ReCp^*(CO)_3$, **3**, Cp* = ($\eta^5$- $C_5Me_5$), in $CH_2Cl_2$/WCEA electrolytes. The radical cation

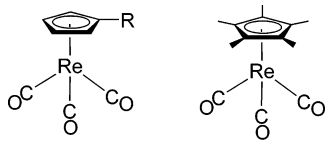


$\mathbf{1}^+$ does, indeed, form positively charged adducts with one-electron donors, allowing the metal to return to its 18-electron, Re(I), electronic state. In the absence of other agents, the radical $\mathbf{1}^+$ exists in equilibrium with the weakly Re−Re bonded dimeric dication $[Re_2Cp_2(CO)_6]^{2+}$, $\mathbf{1}_2^{2+}$. The former is shown to function as a strong one-electron oxidant and to be capable of initiating homolytic cleavage reactions of C−H and C−halogen bonds. DFT calculations and X-ray crystallographic results are reported which delineate electronic and structural properties of this Re system. A preliminary account of the work has appeared.[11]

## 2. Experimental Section

Experimental procedures were performed under nitrogen using either standard Schlenk conditions or a Vacuum Atmospheres drybox. Reagent-grade dichloromethane and 1,2-dichloroethane were twice distilled from $CaH_2$, the second distillation being carried out, bulb-to-bulb, under static vacuum. Other solvents were purified and dried by distillation from potassium (diethyl ether, hexanes, and pentane) or potassium benzophenone (THF).

The moisture sensitivity of the dimer dications required that particularly close attention be paid to the dryness of the solvents and glass vessels employed. NMR solvents were used as received from CIL ($CD_2Cl_2$) or Acros ($CD_3NO_2$). Glassware used for electrochemical experiments was cleaned in aqua regia, followed by copious rinsings by nanopure water and subsequent drying for at least 12 h in a 120 °C oven. The warm glassware was loaded into the drybox antechamber and allowed to cool under vacuum. Ferrocene, $ReCp(CO)_3$, **1**, and $ReCp^*(CO)_3$, **3** (Cp* = $\eta^5$-$C_5Me_5$), were purchased from Strem Chemical Co. and used as received. The supporting electrolytes, $[NBu_4][PF_6]$[9a] and $[NBu_4][TFAB]$[10b] (TFAB = $[B(C_6F_5)_4]$), were prepared as previously described, the latter being metathesized from alkali metal salts purchased from Boulder Scientific Co.

**2.1. $Re(C_5H_4NH_2)(CO)_3$, 2.** Although this compound had been reported earlier by Nesmeyanov et al.,[12a] the improved approach to aminocyclopentadienyl complexes used by Barybin et al.[12b] for the preparation of $Mn(C_5H_4NH_2)(CO)_3$ was adapted here for synthesis of the rhenium analogue. After cooling a solution of 0.20 g (0.60 mmol) of $ReCp(CO)_3$ in 3.2 mL of THF to 195 K, 0.4 mL (0.64 mmol) of *n*-BuLi (Acros, 1.6 M in hexanes) was added with stirring. After 50 min, 0.25 g (1.27 mmol) of tosyl azide[12c] was added, and the resulting solution was allowed to warm to room temperature over the course of 1 h, followed by stirring for an additional 12 h. At this point an NMR spectrum was obtained which indicated the presence of the cyclopentadienyl azide complex ($^1$H NMR ($CD_2Cl_2$): $\delta$ (ppm vs TMS) 5.33 (t, 2H), 5.22 (t, 2H)). The solvent was removed *in vacuo*, and the remaining brown solid was dissolved in 4.0 mL of 95% EtOH. To this was slowly added 0.095 g (2.51 mmol) of $NaBH_4$ in 3.5 mL of 95% EtOH, during which an exothermic reaction was evident. After 45 min, the solvent was removed and the light brown solid was extracted with 4 × 20 mL of diethyl ether. Evaporation gave a white solid that contained a mixture of starting material and **2**. Recrystallization from $CH_2Cl_2$/hexanes gave pure **2** in 83−94 mg (40−45%) yield. Anal. Calcd for **2**: C, 27.51; H, 1.73; N, 4.01. Found: C, 27.65; H, 1.66; N, 3.89. IR ($CH_2Cl_2$): $\nu_{CO}$ 2017 vs, 1919 vs cm$^{-1}$. $^1$H NMR ($CD_2Cl_2$): $\delta$ (ppm vs TMS) 4.99 (t, 2H), 4.87 (t, 2H), 3.31 (broad s, 2H).

**2.2. $[ReCp(CO)_3Cl][B(C_6F_5)_4]$, 4[TFAB].** This salt was prepared by metathesis of the corresponding hexachloroantimonate complex, which had been synthesized from **1** according to the literature method.[12d] To 90 mg (0.13 mmol) of $[ReCp(CO)_3Cl][SbCl_6]$ in 5 mL of spectrograde nitromethane 90 mg (0.12 mmol) of $K[B(C_6F_5)_4]$ in 5 mL of nitromethane were added dropwise, with stirring, over 10 min, giving a homogeneous yellow solution. The solid remaining after vacuum evaporation was extracted with 10 mL of $CH_2Cl_2$, followed by filtration through Celite. Evaporation of the resulting filtrate provided a yellow-orange powder which was recrystallized from $CH_2Cl_2$/hexanes, giving 120 mg (90%) of [**4**][$B(C_6F_5)_4$]. IR ($CH_2Cl_2$,) $\nu_{CO}$ : 2139, 2084 cm$^{-1}$; $\nu(B(C_6F_5)_4)$: 1643, 1515, 1461, 1275, 1080, 979 cm$^{-1}$. $^1$H NMR ($CD_2Cl_2$): $\delta$ (ppm vs TMS) 6.56 (s). Anal. Calcd for $[ReCp(CO)_3Cl][TFAB]$: C, 36.61; H, 0.48. Found: C, 36.70; H, 0.59.

(6) (a) Adams, R. D.; Collins, D. E.; Cotton, F. A. *J. Am. Chem. Soc.* **1974**, *96*, 749. (b) Landrum, J. T.; Hoff, C. D. *J. Organomet. Chem.* **1985**, *282*, 215. (c) Hackett, P.; O'Neill, P. S.; Manning, A. R. *J. Chem. Soc., Dalton Trans.* **1974**, 1625. (d) Madach, T.; Vahrenkamp, H. *Z. Naturforsch.* **1979**, *34b*, 573. (e) Goh, L.-Y.; D' Aniello, M. J.; Slater, S.; Muetterties, E. L.; Tavanaiepour, I.; Chang, M. I.; Fredrich, M. F.; Day, V. W. *Inorg. Chem.* **1979**, *18*, 192. (f) Cooley, N. A.; Watson, K. A.; Fortier, S.; Baird, M. C. *Organometallics* **1986**, *5*, 2563. (g) Keller, H. J. *Z. Naturforsch.* **1968**, *23b*, 133. (h) Madach, T.; Vahrenkamp, H. *Z. Naturforsch.* **1978**, *33b*, 1301. (i) McLain, S. J. *J. Am. Chem. Soc.* **1988**, *110*, 643. (j) Cooley, N. A.; MacConnachie, P. T. F.; Baird, M. C. *Polyhedron* **1988**, *7*, 1965. (k) Jaeger, T. J.; Baird, M. C. *Organometallics* **1988**, *7*, 1965. (l) Wrighton, M. S.; Ginley, D. S. *J. Am. Chem. Soc.* **1975**, *97*, 4246. (m) Hughey, J. L.; Bock, C. R.; Meyer, T. J. *J. Am. Chem. Soc.* **1975**, *97*, 4440. (n) Laine, R. M.; Ford, P. C. *Inorg. Chem.* **1977**, *16*, 388. (o) Watkins, W. C.; Jaeger, T.; Kidd, C. E.; Fortier, S.; Baird, M. C.; Kiss, G.; Roper, G. C.; Hoff, C. D. *J. Am. Chem. Soc.* **1992**, *114*, 907. (p) Goh, L. Y.; Habley, T. W.; Darensbourg, D. J.; Reibenspies, J. *J. Organomet. Chem.* **1990**, *381*, 349. (q) Lin, G.; Wong, W.-T. *J. Organomet. Chem.* **1996**, *522*, 271. (r) Clegg, W.; Compton, N. A.; Errington, R. J.; Norman, N. C. *Acta Crystallogr.* **1988**, *C44*, 568. (s) Rheingold, A. L.; Harper, J. R. *Acta Crystallogr.* **1991**, *C47*, 184. (t) Richards, T. C.; Geiger, W. E.; Baird, M. C. *Organometallics* **1994**, *13*, 4494. (u) Woska, D. C.; Ni, Y.; Wayland, B. B. *Inorg. Chem.* **1999**, *38*, 4135. (v) O' Callaghan, K. A. E.; Brown, S. J.; Page, J. A.; Baird, M. C.; Richards, T. C.; Geiger, W. E. *Organometallics* **1991**, *10*, 3119. (w) Yao, Q.; Bakac, A.; Espenson, J. H. *Organometallics* **1993**, *12*, 2010. (x) Kadish, K. M.; Lacombe, D. A.; Anderson, J. E. *Inorg. Chem.* **1986**, *25*, 2246. (y) Brownie, J. H.; Baird, M. C.; Laws, D. R.; Geiger, W. E. *Organometallics* **2007**, 26, 5890.

(7) (a) Alvarez, M. A.; García, G.; García, E.; Riera, V.; Ruiz, M. A.; Lanfranchi, M.; Tiripicchio, A. *Organometallics* **1999**, *18*, 4509. (b) Beck, W.; Sünkel, K. *Chem. Rev.* **1988**, *88*, 1405. (c) Camire, N.; Nafady, A.; Geiger, W. E. *J. Am. Chem. Soc.* **2002**, *124*, 7260.

(8) *Dileptic* describes the metal complex as containing only two types of ligands (Cp and CO in this case) and emphasizes its "parental", i.e., unsubstituted, character. For a recent review on *homo*leptic metal carbonyl cations, see: Xu, Q. *Coord. Chem. Rev.* **2002**, *231*, 83.

(9) Nafady, A.; Costa, P. J.; Calhorda, M. J.; Geiger, W. E. *J. Am. Chem. Soc.* **2006**, *128*, 16587.

(10) (a) Barriére, F.; Geiger, W. E. *J. Am. Chem. Soc.* **2006**, *128*, 3980. (b) LeSuer, R. J.; Buttolph, C.; Geiger, W. E. *Anal. Chem.* **2004**, *76*, 6395. (c) Camire, N.; Mueller-Westerhoff, U. T.; Geiger, W. E. *J. Organomet. Chem.* **2001**, *637*−*639*, 823. (d) LeSuer, R. J.; Geiger, W. E. *Angew. Chem., Int. Ed.* **2000**, *39*, 248. (e) Hill, M. G.; Lamanna, W. M.; Mann, K. R. *Inorg. Chem.* **1991**, *30*, 4687.

(11) Chong, D.; Nafady, A.; Costa, P. J.; Calhorda, M. J.; Geiger, W. E. *J. Am. Chem. Soc.* **2005**, *127*, 15676.

(12) (a) Nesmeyanov, A. N.; Anisimov, K. N.; Kolobova, N. E.; Markarov, Yu. V. *Izvetiya Akademii Nauk SSSR, Seriya Khimicheskaya* **1968**, *6*, 1421. (b) Holovics, T. C.; Deplazes, S. F.; Toriyama, M.; Powell, D. R.; Lushington, G. H.; Barybin, M. V. *Organometallics* **2004**, *23*, 2927. (c) Regitz, M.; Hocker, J.; Liedhegener, A. *Org. Synth.* **1973**, *5*, 179. (d) King, R. B. *J. Inorg. Nucl. Chem.* **1967**, *29*, 2119.

**2.3. $[Re_2Cp_2(CO)_6][B(C_6F_5)_4]_2$, $[\mathbf{1_2}][TFAB]_2$.** 37 mg (0.11 mmol) of $ReCp(CO)_3$ in 15 mL of $CH_2Cl_2$/0.05 M $[NBu_4][B(C_6F_5)_4]$ were added to the working electrode compartment (see electrochemical section below) and electrolyzed, with stirring, using $E_{appl} = 1.3$ V at 243 K. The reduced temperature takes advantage of the poor solubility of the product at this temperature, allowing the yellow dimer dication to precipitate as the oxidation proceeds. The progress of the electrolysis was followed by coulometry, which required precisely 1.0 F for completion. At that point, the only product waves observed in CV scans were those of the slightly soluble $\mathbf{1_2}^{2+}$ ($E_{pc} = 0.55$ V, scan rate 0.2 V $s^{-1}$) and the soluble side product $[ReCp(CO)_3Cl]^+$, **4** ($E_{pc} = -0.16$ V). The contents of the working electrode compartment were then filtered through a fine glass frit and washed three times with 4 mL portions of cold $CH_2Cl_2$, providing 78 to 89 mg (70−80%) of analytically pure $[\mathbf{1_2}][TFAB]_2$, which was stable indefinitely if kept in the drybox at room temperature. Electrolyses were also conducted on a slightly larger scale, starting with about 60 mg of **1**, with somewhat lower yields (*ca.* 55−65%) of dimer. In this case, precipitation onto the platinum gauze caused periodic electrode passivation, typically two or three times during the electrolysis, at which time the working electrode was removed and cleaned by rinsing it with $CH_2Cl_2$ or $C_2H_4Cl_2$ at ambient temperature. Anal. Calcd for $[\mathbf{1_2}][TFAB]_2$: C, 37.88; H, 0.50. Found: C, 37.55; H, 0.50. IR ($CH_2Cl_2$): $\nu_{CO}$ 2105, 2031 $cm^{-1}$; IR (nujol): $\nu_{CO}$ 2113, 2098, 2046, 2037 $cm^{-1}$. $^1H$ NMR ($CD_2Cl_2$): $\delta$ (ppm vs TMS) 6.40 (s).

**2.4. $[Re_2(C_5H_4NH_2)_2(CO)_6][B(C_6F_5)_4]_2$, $[\mathbf{2_2}][TFAB]_2$.** An electrolytic procedure at 243 K using $E_{appl} = 1.0$ V, but otherwise similar to that detailed above for $[\mathbf{1_2}]$ $[TFAB]_2$, gave 50−60% yield of the pure yellow dimer $[\mathbf{2_2}][TFAB]_2$. The electrolysis solution commonly became supersaturated with the dimer dication, and a way around this slow precipitation of the desired product was found by happenstance (see discussion in text). Anal. Calcd: C, 37.33; H, 0.59; N, 1.36. Found: C, 36.80; H, 0.84; N, 1.40. IR ($C_2H_4Cl_2$): $\nu_{CO}$ 2071, 2007 (with asymmetry on high-frequency side) $cm^{-1}$. IR (KBr): $\nu_{CO}$ 2083 vs, 2022 sh, 2012 vs $cm^{-1}$. $^1H$ NMR ($CD_3NO_2$): $\delta$ (ppm vs TMS) 6.54 (broad s, 4H), 6.22 (t, 4H), 5.47 (t, 4H). X-ray quality crystals of $[\mathbf{2_2}][TFAB]_2$ were grown from a solution of the dimer dication in nitromethane, to which a small amount of dichloromethane had been added until the first observed level of cloudiness. Kept overnight at 253 K, the desired crystals were obtained.

**2.5. $[Re_2Cp^*_2(CO)_6][B(C_6F_5)_4]_2$, $[\mathbf{3_2}][TFAB]_2$.** As 50 mg of $ReCp^*(CO)_3$ dissolved in 10 mL of $CH_2Cl_2$/0.05 M $[NBu_4][TFAB]$ were electrolyzed at 243 K, $E_{appl} = 1.1$ V, the solution turned deep yellow. Near the end of the electrolysis, when the current was only a few % of its initial value, precipitation of the yellow-orange solid occurred. After being kept cold for another 20 min, the solution was filtered and washed with cold $CH_2Cl_2$ and hexanes to remove electrolyte and any unreacted starting material. Evaporation gave 105 mg (79%) of analytically pure $[Re_2Cp^*_2(CO)_6][TFAB]_2$. $\nu_{CO}(CH_2Cl_2) = 2062, 2018, 2010$ $cm^{-1}$, Anal. Calcd: C, 40.97; H, 1.38. Found: C, 40.76; H 1.28.

**2.6. $[Fe(C_5H_4COCH_3)_2][B(C_6F_5)_4]$.** To a solution of 19 mg (7.0 $\mu$mol) of bis(acetylcyclopentadienyl)iron (Aldrich) in 1 mL of $CH_2Cl_2$ a solution of 7 mg (3.45 $\mu$mol) of $[Re_2Cp_2(CO)_6][B(C_6F_5)_4]_2$ in 2 mL of $CH_2Cl_2$ was added slowly, with stirring, at 263 K. An immediate color change from orange to green occurred. The solvent was removed *in vacuo* to provide a green solid which was washed 10 times with *n*-hexane to remove $ReCp(CO)_3$ and any of the unreacted ferrocene derivative. Vacuum evaporation provided 59 mg (89%) of analytically pure green microcrystals of $[Fe(C_5H_4COCH_3)_2][B(C_6F_5)_4]$. Anal. Calcd. for $C_{38}H_{14}O_2F_{20}BFe$: C, 48.08; H, 1.49. Found: C, 47.95; H, 1.60. $\lambda_{max}$ ($CH_2Cl_2$) = 656 nm ($\epsilon = 270$ $M^{-1}$ $cm^{-1}$). IR (nujol): $\nu_{CO}$ 1686 $cm^{-1}$ (lit.: 1687 $cm^{-1}$).[13]

**2.7. Electrochemistry.** A standard three-electrode configuration was employed in conjunction with a PARC 273A potentiostat interfaced to a personal computer through homemade software. IR spectroelectrochemistry was carried out under Schlenk-type conditions, and other electrochemical experiments were conducted inside a Vacuum Atmospheres drybox, which was outfitted with a cooling bath capable of controlling solution temperatures to about 1 °C. Oxygen levels in the drybox were typically 1−5 ppm during the course of an experiment. Bulk electrolyses were carried out in a three-compartment "H-type" cell having counter and working compartments separated by a fine glass frit. The working electrode was a basket-shaped Pt gauze which had been treated with nitric acid, washed copiously with distilled water, and dried by first leaving it overnight at 120 K, followed by evacuation. Voltammetry scans were recorded using a glassy carbon working electrode disk of either 1 or 2 mm diameter (Bioanalytical Systems), the effective areas of which were checked by chronoamperometric measurements of ferrocene in acetonitrile/0.1 M $[NBu_4][PF_6]$, for which a diffusion coefficient of $2.4 \times 10^{-5}$ $cm^2$ $s^{-1}$ has been reported.[14] The disks were pretreated using a standard sequence of polishing with diamond paste (Buehler) of decreasing sizes (3 to 0.25 $\mu$m) interspersed by washings with nanopure water, and finally vacuum drying. All potentials given in this paper are referred to the ferrocene (FcH)/ferrocenium reference couple.[15] Mechanistic aspects of redox reactions were probed by applying the appropriate diagnostic criteria to cyclic voltammetry (CV) data, using procedures described elsewhere.[16]

**2.8. Digital Simulations.** Digital simulations of the background-subtracted and iR-compensated CV data for compounds **1**−**3** were performed using Digisim 3.0 (Bioanalytical Systems). Fitting the initial anodic process involving the one-electron oxidation (e.g., $\mathbf{1}/\mathbf{1}^+$) and coupled dimerization (e.g., $2\ \mathbf{1}^+ \rightarrow \mathbf{1_2}^{2+}$), an $EC_{dim}$ process, gave reliable values for $E_{1/2}$ and the lower limit of $K_{dim}$ (*vide infra*; see discussion of simulations for **1**). The reverse cathodic feature, arising from the reduction of the dimer dication $\mathbf{1_2}^{2+}$ back to the starting material **1**, was only simulated for the purpose of having a reasonable visual fit. As seen in the figures to follow, this cathodic feature was broad and highly electrochemically irreversible. It almost certainly involves a net transfer of two electrons, most likely through an $E_{irrev}C_{irrev}E$ mechanism, in which the chemical step, $C_{irrev}$, is cleavage of the Re−Re bond in an intermediate dimer monocation $\mathbf{1_2}^+$. It is not likely that a unique fit of the electrochemical and chemical parameters could be found for such a mechanism. Therefore we modeled these cathodic back-reactions with the simpler $E_{irrev}E$ model, using values for $E_{irrev}$ that befit a very slow charge-transfer rate ($k_s$ ca. $10^{-5}$ cm $s^{-1}$), with charge-transfer coefficients ($\alpha$) less than 0.5 (typically, 0.3 to 0.35) and diffusion coefficients for $\mathbf{1_2}^{2+}$ and the other dimers that simply fit with the observed cathodic peak currents and shapes. Only the values derived for the initial $EC_{dim}$ process should be taken to have quantitative significance.

**2.9. Spectroscopy.** IR spectra were recorded with an ATI-Mattson Infinity Series FTIR interfaced to a computer employing Winfirst software at a resolution of 4 $cm^{-1}$, and NMR spectra were recorded using a Bruker ARX 500 MHz spectrometer. *In situ* IR spectroelectrochemistry[17] was performed using a mid-IR fiber-optic "dip" probe (Remspec, Inc) with a standard H-type electrolysis cell under argon. In these experiments, the bulk electrolysis was intermittently halted at selected Coulombic points in order to record the spectrum of the electrolysis solution. The spectra typically took 2 to 3 min to record, after which the electrolysis was continued to another stopping point until the electrolysis current was 1% or less of the original value. UV−vis spectra were recorded with an Olis Cary-14 spectrometer.

**2.10. X-ray Crystallography.** Crystallographic data are collected in Table 1. Data were collected on a Bruker D8 platform diffractometer equipped with an APEX CCD detector. The structure was solved by a

(13) Guillon, C.; Vierling, P. *J. Organomet. Chem.* **1994**, *464*, C42.
(14) Hershberger, J. W.; Klingler, R. J.; Kochi, J. K. *J. Am. Chem. Soc.* **1983**, *105*, 61.
(15) (a) Gritzner, G.; Kuta, J. *Pure Appl. Chem.* **1984**, *56*, 461. (b) Connelly, N. G.; Geiger, W. E. *Chem. Rev.* **1996**, *96*, 877.
(16) Geiger, W. E. In *Laboratory Techniques in Electrochemistry*, 2nd ed.; Kissinger, P. T., Heineman, W. R., Eds.; Marcel Dekker: New York, 1996; Chapter 23.
(17) Shaw, M. J.; Geiger, W. E. *Organometallics* **1996**, *15*, 13.

**Table 1.** Crystal Data and Structure Refinement for $[\mathbf{2_2}][TFAB]_2 \cdot 2H_2O$

| | | |
|---|---|---|
| empirical formula | $C_{64}H_{12}B_2F_{40}N_2O_6Re_2 \cdot 2H_2O$ | |
| formula weight | 2094.82 | |
| temperature | 100(2) K | |
| crystal system | triclinic | |
| space group | $P\bar{1}$ | |
| unit cell dimensions | $a = 11.9709(5)$ Å | $\alpha = 94.268(1)°$ |
| | $b = 12.1176(5)$ Å | $\beta = 92.209(1)°$ |
| | $c = 12.3692(6)$ Å | $\gamma = 118.233(1)°$ |
| volume | 1570.85(12) Å$^3$ | |
| $Z$ | 1 | |
| density (calculated) | 2.214 g/cm$^3$ | |
| absorption coefficient (Mo Kα) | 4.031 mm$^{-1}$ | |
| $F(000)$ | 998 | |
| crystal size | 0.31 × 0.21 × 0.11 mm$^3$ | |
| crystal color, habit | yellow, plate | |
| $\theta$ range for data collection | 1.66 to 28.31° | |
| reflections collected | 13063 | |
| independent reflections | 6866 [$R$(int) = 0.0215] | |
| data/restraints/parameters | 6866/3/544 | |
| goodness-of-fit on $F^2$ | 1.065 | |
| final $R$ indices [$I > 2\sigma(I)$] | $R1 = 0.0241$, $wR2 = 0.0607$ | |
| $R$ indices (all data) | $R1 = 0.0257$, $wR2 = 0.0616$ | |
| largest diff. peak and hole | 1.552 and −0.712 e Å$^{-3}$ | |

Patterson projection. All non-hydrogen atoms were refined anisotropically, and the hydrogen atoms, except for those on the water molecule, were placed in idealized locations. The asymmetric unit contained two molecules of water from unknown sources for each Re dimer. The hydrogen atoms on the unique water molecule were located, and the geometry of the water molecule was restrained during refinement. All software was contained in the SMART, SAINT, and SHELXTL libraries distributed by Bruker AXS, Madison, WI.

**2.11. DFT Calculations.** All Density Functional Theory calculations[18] were performed using the Amsterdam Density Functional program package (ADF, versions 2004 and 2005).[19] Gradient corrected geometry optimizations[20] (gas-phase and solvent) were performed without symmetry constraints using the Local Density Approximation of the correlation energy (Vosko−Wilk−Nusair),[21a] augmented by the exchange-correlation functional of Perdew−Wang (PW91).[21b] Triple-ζ Slater-type orbitals (STOs) were used to describe the valence shells of C, O, H, and Re, with a set of two polarization functions (p,f for Re; d,f for C, O; and p,d for H). The core orbitals were frozen for Re ([1−4]s, [2−4]p, [3−4]d), C, and O (1s). The relativistic effects were treated with the ZORA approximation.[22] The solvent effects were included using the COnductor like Screening MOdel (COSMO)[23] implemented in ADF. The rigid sphere radius of the $CH_2Cl_2$ solvent molecules was taken to be 2.449 Å,[24] and the dielectric constant was 8.93. The van der Waals radii of the atoms were used for the atomic radius of the solute (or atomic radius in the case of Re): Re, 1.370 Å; C, 1.700 Å; O, 1.520 Å; H, 1.200 Å.[25] The oxidation potentials were calculated as described elsewhere.[9] Free energy changes ($\Delta G$), as well as inclusion of the zero-point energy (ZPE), should be considered for the $M \rightarrow M^+ + e^-$ reaction and for the calculation of dimerization energies. This requires, however, the demanding computation of the vibrational frequencies. As Ziegler has shown[26] that the electrochemical behavior of cyclooctatetraene is mainly determined by electronic enthalpies, we calculated redox potentials based on electronic enthalpies, rather than free energies. The good agreement between calculated and experimental data validated this approximation. The dimerization energies were also computed based on electronic enthalpies, although the entropic contributions are expected to be relevant for an associative process.

**Table 2.** Listing of $\nu$(CO) Infrared and Redox Potentials for Re Compounds

| | $\nu$(CO)/cm$^{-1}$ | | $E_{1/2}$ | $E_{pc}$ |
|---|---|---|---|---|
| compounds | in $CH_2Cl_2$ | in nujol | V vs $Cp_2Fe^{0/+}$ | |
| **1** | 2024, 1926 | | 1.16 | |
| $\mathbf{1_2}^{2+}$ | 2105, 2031 | 2113, 2098, 2046, 2037 | | 0.55 |
| **2** | 2017,1919 | | 0.79 | |
| $\mathbf{2_2}^{2+}$ | 2071, 2007[a] | 2083, 2012 (in KBr) | | −0.01 |
| **3** | 2005, 1906 | | 0.91 | |
| $\mathbf{3_2}^{2+}$ | 2062, 2015 | 2062, 2015 | | 0.15 |
| **4** | 2140, 2085 | | | −0.16 |

[a] These data were obtained in dichloroethane, in which the dimer dication is more soluble. Values of 2076 and 2010 cm$^{-1}$ were obtained *in situ* when $\mathbf{2_2}^{2+}$ was electrolytically generated in $CH_2Cl_2$, and these values were used to compute the raw carbonyl shift discussed in the text.

## 3. Results and Discussion

**3.1. General Anodic Behavior.** The half-sandwich complexes **1**−**3** share the same primary voltammetric characteristic, namely a partly chemically reversible one-electron oxidation at fairly positive potentials which gives, in addition to the radical cation, a product having a broad and irreversible cathodic wave about 0.6 to 0.8 V negative of the original anodic wave. The characteristics of the voltammetry vary with changes in temperature, scan rate, and concentrations of the analyte, arising, as will be shown below, from an $EC_{dim}$ process (eqs 1 and 2) for the anodic wave and an overall two-electron, electrochemically irreversible, process (eq 3) for the cathodic wave.

$$ReCp^{\gamma}(CO)_3 - e^- \rightleftharpoons [ReCp^{\gamma}(CO)_3]^+ \qquad E_{1/2} \quad (1)$$

where $Cp^{\gamma}$ = Cp (**1**), $C_5H_4(NH_2)$ (**2**), or Cp* (**3**)

$$2\,[ReCp^{\gamma}(CO)_3]^+ \rightleftharpoons [Re_2Cp^{\gamma}{}_2(CO)_6]^{2+} \qquad K_{dim} \quad (2)$$

$$[Re_2Cp^{\gamma}{}_2(CO)_6]^{2+} + 2\,e^- \rightarrow 2\,ReCp^{\gamma}(CO)_3 \qquad E_{pc} \quad (3)$$

Although the monomer/dimer equilibrium (eq 2) lies in favor of the latter, partial dissociation of the dimer gives, at least for the Cp and Cp* complexes, modest amounts (several percent, depending on temperature and concentration) of the very reactive 17 e$^-$ monomeric cation radical. The dimer dications, which have Re−Re bonded 18 e$^-$ metal centers unsupported by bridging ligands, are fully characterized, isolable, species. Relevant electrochemical potentials and infrared frequencies are collected in Table 2.

(18) Parr, R. G.; Young, W. *Density Functional Theory of Atoms and Molecules*; Oxford University Press: New York, 1989.
(19) (a) te Velde, G.; Bickelhaupt, F. M.; van Gisbergen, S. J. A.; Guerra, C. F.; Baerends, E. J.; Snijders, J. G.; Ziegler, T. *J. Comput. Chem.* **2001**, *22*, 931. (b) Guerra, C. F.; Snijders, J. G.; te Velde, G.; Baerends, E. J. *Theor. Chem. Acc.* **1998**, *99*, 391. (c) ADF2005.01, SCM, Theoretical Chemistry, Vrije Universiteit, Amsterdam, The Netherlands, http://www.scm.com.
(20) (a) Versluis, L.; Ziegler, T. *J. Chem. Phys.* **1988**, *88*, 322. (b) Fan, L.; Ziegler, T. J. *Chem. Phys.* **1991**, *95*, 7401.
(21) (a) Vosko, S. H.; Wilk, L.; Nusair, M. *Can. J. Phys.* **1980**, *58*, 1200. (b) Perdew, J. P.; Chevary, J. A.; Vosko, S. H.; Jackson, K. A.; Pederson, M. R.; Singh, D. J.; Fiolhais, C. *Phys. Rev.* **1992**, *B46*, 6671.
(22) van Lenthe, E.; Ehlers, A.; Baerends, E. J. *J. Chem. Phys.* **1999**, *110*, 8943.
(23) (a) Klamt, A.; Schüürmann, G. *J. Chem. Soc., Perkin Trans.* **1993**, *2*, 799. (b) Klamt, A. *J. Phys. Chem.* **1995**, *99*, 2224. (c) Klamt, A.; Jones, V. *J. Chem. Phys.* **1996**, *105*, 9972. (c) Pye, C. C.; Ziegler, T. *Theor. Chem. Acc.* **1999**, *101*, 396.
(24) Reid, R. C.; Prausnitz, J. M.; Poling, B. E. *The Properties of Gases and Liquids*, 4th ed.; McGraw-Hill International: 1987; Appendix B pp 733−734.
(25) Bondi, A. *J. Phys. Chem.* **1964**, *68*, 441.
(26) Baik, M-H.; Schauer, C. K.; Ziegler, T. *J. Am. Chem. Soc.* **2002**, *124*, 11167.

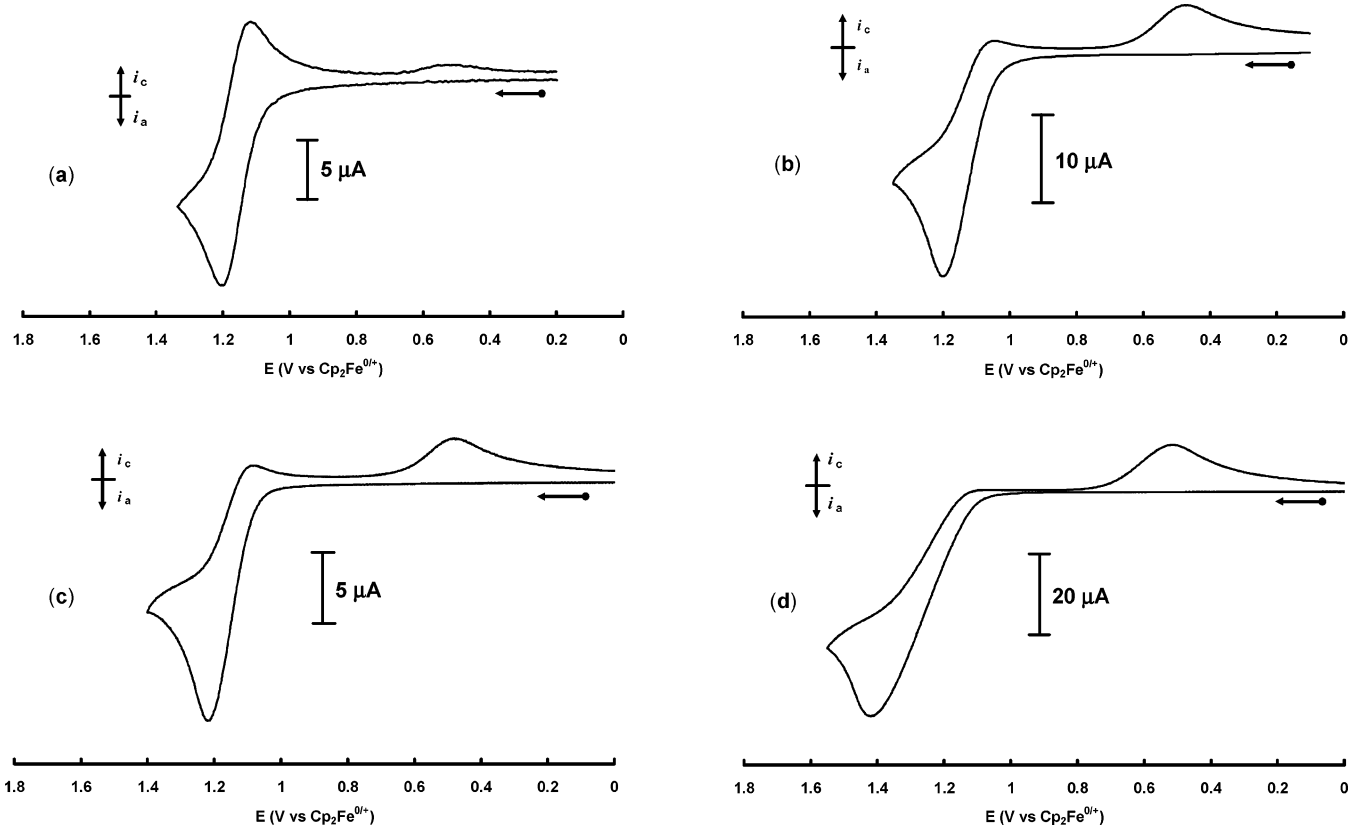


***Figure 1.*** Cyclic voltammograms (CVs) of **1** in $CH_2Cl_2$/0.05 M $[NBu_4][TFAB]$ at 1 mm glassy carbon electrode (gce), under various conditions of concentration of **1**, scan rate, and temperature: (a) 0.64 mM, 1 V $s^{-1}$, 273 K; (b) 1.5 mM, 0.2 V $s^{-1}$, 298 K; (c) 1.0 mM, 0.2 V $s^{-1}$, 243 K; and (d) 5 mM, 0.2 V $s^{-1}$, 295 K. There is significant ohmic distortion at the highest concentration (d).

**3.1.1. $ReCp(CO)_3$, 1.** Figure 1, which gives a sampling of CV scans taken at different scan rates for varying analyte concentrations, is representative of the voltammetric behavior of this family of compounds, wherein the observed chemical reversibility of the $[ReCp(CO)_3]^{0/+}$ couple ($E_{1/2}$ = 1.16 V) decreases at slower scan rates (Figure 1b) and higher analyte concentrations (Figure 1d, distorted by ohmic loss). The effect of temperature changes on the chemical reversibility of $\mathbf{1}/\mathbf{1}^+$ is more complex, owing to competition between the kinetic and thermodynamic aspects of the dimerization. Generally, however, the irreversible cathodic wave for the dimer is enhanced at lower temperatures (see Figure 1c, a slow-scan CV of 1 mM **1** at 243 K). The position ($E_{pc}$) and peak width ($\delta E_p = E_p - E_{p/2}$) of this cathodic wave for the reduction of the dimer dication $\mathbf{1}_2^{2+}$ back to **1** are quite temperature and scan rate dependent, consistent with the behavior of an electrochemically irreversible process,[27] with values of $E_{pc}$ = 0.55 V and $\delta E_p$ = 97 mV being observed for $\upsilon$ = 0.2 V $s^{-1}$ at ambient temperatures.

There are significant limitations in determining equilibrium constants for reversible chemical follow-up reactions which strongly favor the follow-up product, as is the case in the present monomer/dimer equilibrium. Focusing on the oxidation of **1**, the key voltammetric measureable is the degree of chemical reversibility of the $\mathbf{1}/\mathbf{1}^+$ anodic/cathodic pair, which is small under our experimental conditions. This analytical problem is not ameliorated by measurement of the height of the cathodic wave of the follow-up product ($\mathbf{1}_2^{2+}$), which does not easily inform us about the concentration of the dimer dication (see Experimental Section). We therefore approached the digital simulations with two goals in mind: to obtain the value of $K_{dim}$ giving the *optimum fit* with experiment and to also find the *highest value* of $K_{dim}$ that *failed* to fit the experimental data. The former values are given as the "determined" dimerization equilibrium constants in Table 3, and the latter are quoted in the text as the *lower limits* of $K_{dim}$. For the Cp compound, a value of $K_{dim} = 10^6$ $M^{-1}$ (Figure 2) gave optimal results, $K_{dim} = 10^5$ $M^{-1}$ (lower limit) gave fits that were still judged to be within experimental error, and $K_{dim} = 10^4$ $M^{-1}$ was clearly too low to account for the experimental data over a range of scan rates.

***Table 3.*** Digital Simulation Parameters for Anodic Processes of **1**, **2**, and **3** at Room Temp

| | $E^o$ (V) | $k_s$ (cm $s^{-1}$) | α | $D_0$ ($cm^2$ $s^{-1}$) | $K_{dim}$ ($M^{-1}$) | $k_{dim}$ ($M^{-1}$ $s^{-1}$) |
|---|---|---|---|---|---|---|
| $\mathbf{1}^{0/+}$ | 1.165 | 0.07 | 0.4 | $2.10 \times 10^{-5}$ | $1.0 \times 10^6$ | $1.0 \times 10^4$ |
| $\mathbf{2}^{0/+}$ | 0.790 | 0.07 | 0.5 | $2.10 \times 10^{-5}$ | $1.0 \times 10^7$ | $1.2 \times 10^5$ |
| $\mathbf{3}^{0/+}$ | 0.905 | 0.05 | 0.4 | $1.73 \times 10^{-5}$ | $1.0 \times 10^5$ | $8.5 \times 10^3$ |

Bulk anodic electrolysis of **1** at $E_{appl}$ = 1.3 V in $CH_2Cl_2$/0.05 M $[NBu_4][TFAB]$ at room temperature passed precisely 1.0 F and resulted in an orange solution having as the dominant voltammetric feature the cathodic wave of the dimer dication at $E_{pc}$ = 0.55 V. When solutions were re-electrolyzed at $E_{appl}$ = 0.3 V, 70−80% of the starting material **1** was regenerated. If the anodic electrolysis was carried out at 243 K, or the solution was cooled to that temperature after an electrolysis at 273 K, a yellow solid was obtained that was analyzed for pure dimer dication, $[\mathbf{1}_2][TFAB]_2$, typically in 70−80% isolated yield. An

(27) Bard, A. J.; Faulkner, L. R. *Electrochemical Methods*, 2nd ed.; John Wiley & Sons: New York, 2000; pp 234 ff.

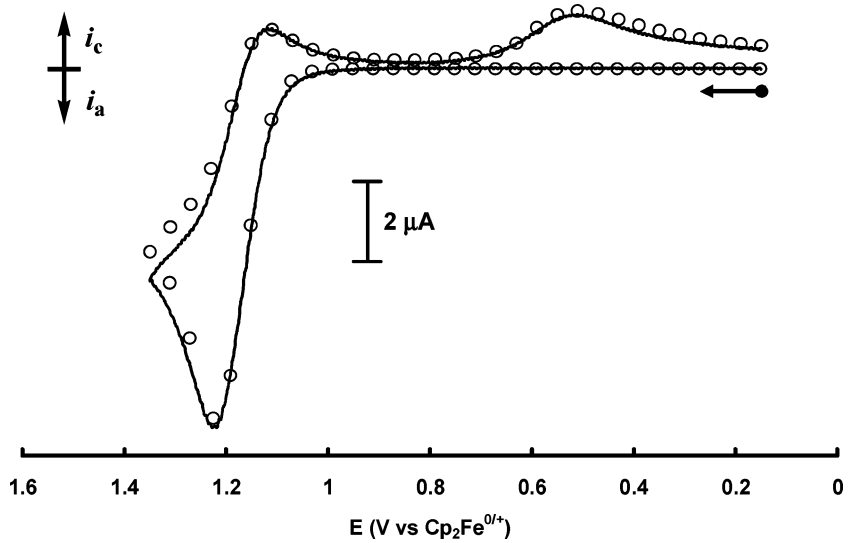


***Figure 2.*** Comparison of experimental (solid) and simulated (circles) CV curves for 1.07 mM **1** in $CH_2Cl_2$/0.05 M [$NBu_4$][TFAB] at 296 K, 1 mm (diam) gce, 0.5 V $s^{-1}$. Important simulation parameters in Table 3.

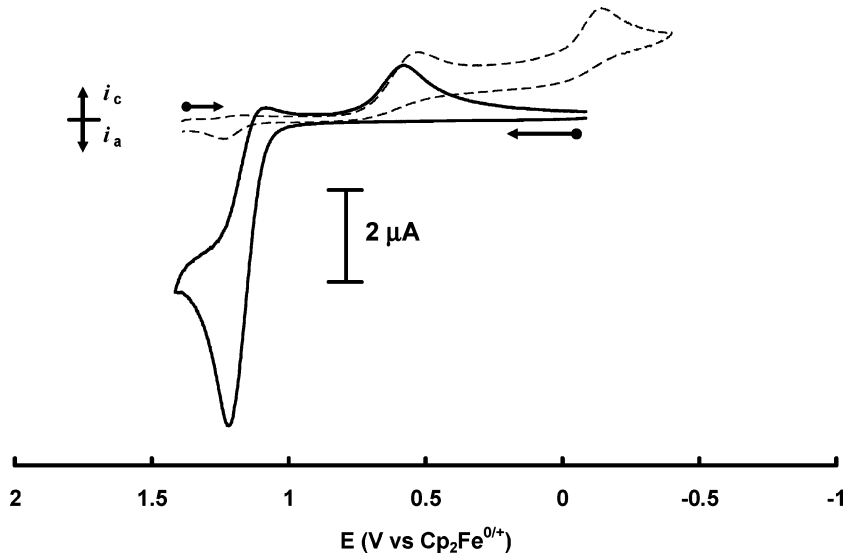


***Figure 3.*** CVs of **1** before electrolysis (arrow pointing left) and after bulk anodic electrolysis at 1.3 V (arrow pointing right), showing cathodic peak for $[ReCp(CO)_3Cl]^+$ side product at $E_{pc} = -0.16$ V. Conditions: 1 mM in **1**, 1 mm gce, scan rate 0.2 V $s^{-1}$, room temperature.

electroactive secondary product ($E_{pc} = -0.16$ V), later shown to be the chloride complex $[ReCp(CO)_3Cl]^+$, **4** (*vide infra*), accounted for no more than 15% of the products at or below 243 K but as much as 30% when the electrolysis was conducted at room temperature and/or over longer time frames (Figure 3). The reaction of $\mathbf{1}^+$ with dichloromethane is described in more detail below. Bulk electrolytic reduction of this secondary product using $E_{appl} = -0.4$ V also regenerated **1**, through the reaction $\mathbf{4} + e^- \rightarrow \mathbf{1} + Cl^{\bullet}$.[28]

The carbonyl-range infrared spectra were investigated under a number of conditions. A nujol mull spectrum (Figure 4) of isolated $[\mathbf{1_2}][TFAB]_2$ showed four absorption bands at 2113, 2098, 2046, and 2037 $cm^{-1}$ which are attributed to a *cis*/*trans* mixture of the dimer dication. Only two bands were observed (2105, 2031 $cm^{-1}$) in $CH_2Cl_2$ (Supporting Information, Figure SM1), most likely arising from the thermodynamically more stable *trans* isomer.[29] A "raw" average shift[30] of + 97 $cm^{-1}$ is therefore observed for the carbonyl bands in going from **1** to $\mathbf{1_2}^{2+}$. A fiber-optic spectroelectrochemical experiment shed further light on the IR properties of the dimer. Electrolysis of a 2 mM solution of **1** at 243 K gave a single product having $\nu_{CO} = 2097$ and 2038 $cm^{-1}$ as the neutral compound was converted to $\mathbf{1_2}^{2+}$, but after completion of about three-fourths of the electrolysis, this pair of bands disappeared (Figure 5), being replaced by a pair at 2105 and 2031 $cm^{-1}$, identical to the those of the isolated product in solution. The original pair at 2097 and 2038 $cm^{-1}$ almost certainly does not arise from the monocation $\mathbf{1}^+$, which is not present in large amounts at this temperature. Since the *in situ* IR−electrochemistry method

(28) The fate of the chlorine atom is unknown. A referee has pointed out that if $Cl^{\bullet}$ is reduced to $Cl^-$ as it is formed, the cathodic reduction of **4** is a net two-electron process.

(29) Room-temperature IR spectra of $[\mathbf{1_2}][TFAB]_2$ in $CH_2Cl_2$ showed that the dimer dication slowly reverted to the neutral complex **1** over a period of a few hours. No other decomposition or side products were observed in this process.

(30) The expression "raw" refers to the fact that we are calculating the simple difference in energies of the two observed bands without taking into account their degeneracies. The symmetric and asymmetric carbonyl stretches for the neutral compounds **1**−**3** are given in Table 2.

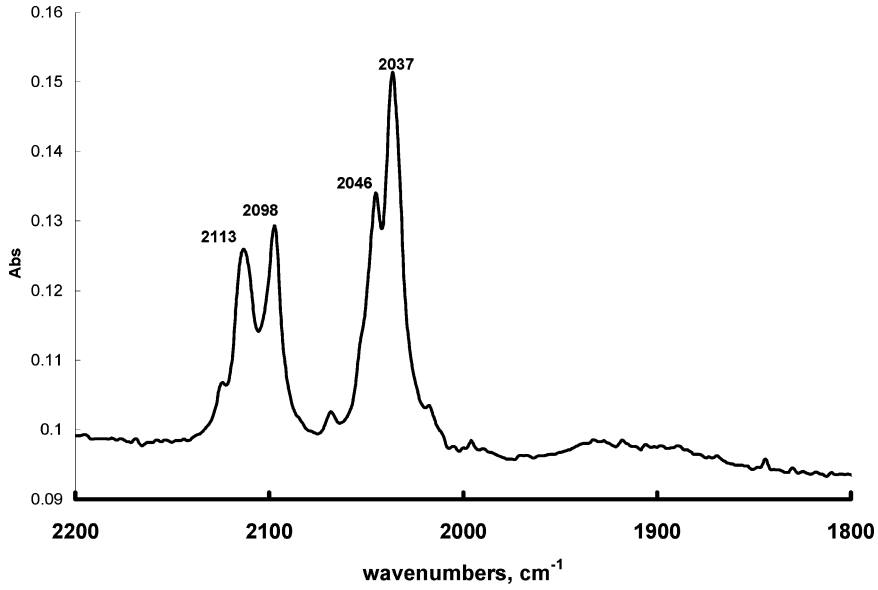


***Figure 4.*** IR spectrum of $[Re_2Cp_2(CO)_6][TFAB]_2$ in nujol.

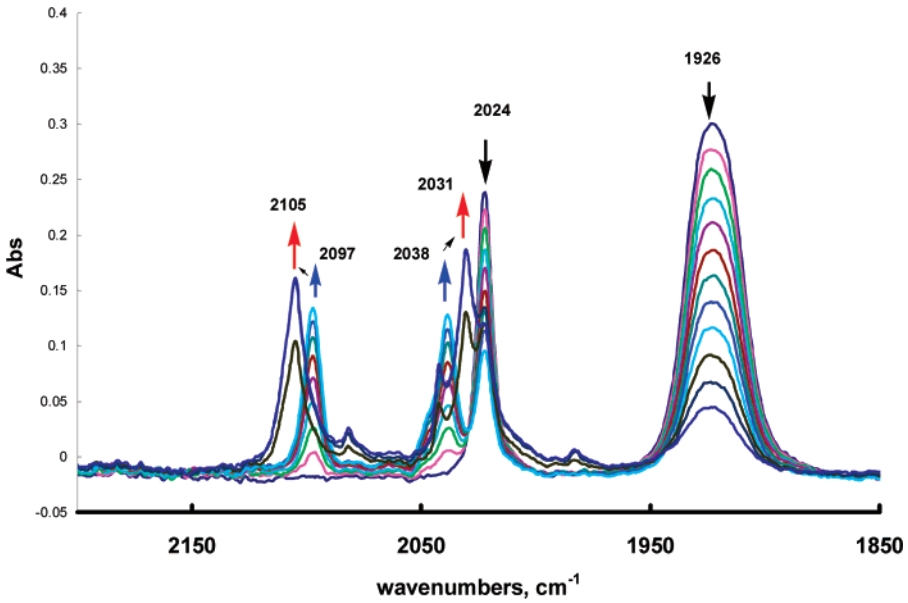


***Figure 5.*** Fiber-optic IR spectra of 2 mM solution of **1** in $CH_2Cl_2$/0.05 M $[NBu_4][TFAB]$ as the anodic electrolysis proceeded at 243 K, $E_{appl} = 1.3$ V. The last spectrum, showing the more intense band at 2105 $cm^{-1}$, is a superposition of the final two spectra recorded in this sequence.

allows for the voltammetric characterization of the electrolysis solution at given points in electrolysis time, we were able to confirm by CV and linear scan voltammetry that the solution contained mostly the dimer dication at the time of recording the next-to-last IR scan of Figure 5 (90% electrolysis). We think it likely that the kinetically favored isomer *cis*-$\mathbf{1}_2^{2+}$ was responsible for the initial pair of CO bands at 2097 and 2038 $cm^{-1}$.

The $^1H$ NMR spectrum of isolated $[\mathbf{1}_2][TFAB]_2$ in $CD_2Cl_2$ gave a sharp resonance at $\delta = 6.40$ ppm. A small singlet at $\delta = 5.33$ ppm was also present, owing to the slow reduction of $\mathbf{1}_2^{2+}$ to **1** at room temperature. Addition of ferrocene to this solution quantitatively reduced the dimer dication to **1**.

**3.1.2. $Re(C_5H_4NH_2)(CO)_3$, 2.** The aminocyclopentadienyl complex **2** also undergoes a one-electron oxidation in $CH_2Cl_2$/$[NBu_4][TFAB]$, with the $\mathbf{2}^{0/+}$ couple differing from $\mathbf{1}^{0/+}$ in terms of oxidation potential ($E_{1/2}$ of 0.79 V, compared to 1.16 V for $\mathbf{1}^{0/+}$) and chemical reversibility (higher scan rates were necessary to observe cathodic reverse currents for $\mathbf{2}^+$). The irreversible cathodic peak for reduction of the dimer dication $\mathbf{2}_2^{2+}$ was observed at $E_{pc} = -0.01$ V (ambient temperature, scan rate 0.1 V $s^{-1}$). Digital simulations (Figure 6) at scan rates from 0.5 to 2 V $s^{-1}$ at 298 K were best fit with values of $K_{dim} = 10^7$ $M^{-1}$ and $k_{dim} = 1.2 \times 10^5$ $M^{-1}$ $s^{-1}$, consistent with the monomer/dimer equilibrium of eq 2 lying slightly more in favor of the dimer for the aminocyclopentadienyl complex compared to its counterparts having either Cp or Cp* (*vide infra*) ligands (for comparative values, see Table 3). A lower limit of $K_{dim} = 10^6$ $M^{-1}$ was obtained for the $\mathbf{2}/\mathbf{2}_2^{2+}$ equilibrium.

Bulk anodic electrolysis of 1.1 mM **2** at $E_{appl} = 0.9$ V in $CH_2Cl_2$/0.06 M $[NBu_4][TFAB]$ at 298 K passed approximately 1.0 F and resulted in a dark yellow solution having as the dominant voltammetric feature the cathodic wave attributed to the dimer dication. The presence of at least two additional minor

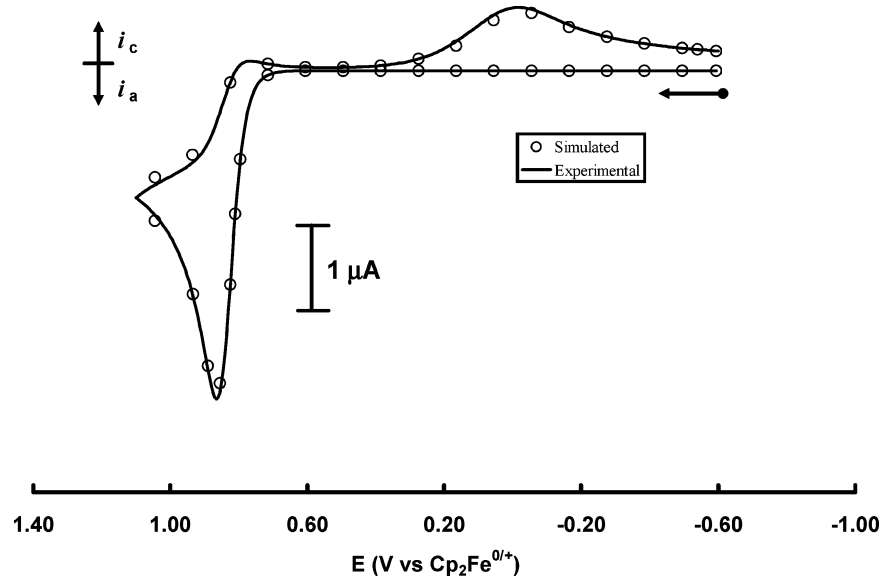


***Figure 6.*** Experimental and simulated CV curves of 0.5 mM **2** in $CH_2Cl_2$/0.1 M $[NBu_4][TFAB]$ at room temperature. The most important parameters are given in Table 3; scan rate = 0.5 V $s^{-1}$.

products was indicated by irreversible cathodic peaks at $E_{pc} = -0.43$ and $-1.18$ V. Infrared spectroscopy of samples removed from this solution showed three significant absorptions in the metal carbonyl range: two high intensity absorptions attributed to $\mathbf{2_2}^{2+}$ at 2076, 2010 $cm^{-1}$ and one weaker band at 2093 $cm^{-1}$, attributed to a side product. Bulk cathodic electrolysis at $E_{appl} = -1.7$ V of the oxidized solution yielded the starting material **2** in about 80% yield, as determined by coulometry and linear scan voltammetry.

Anodic electrolysis using a lower temperature (243 K) and higher (9.6 mM) concentration of **2** allowed isolation of the dimer dication $\mathbf{2_2}^{2+}$. As precisely 1.0 F was passed, a yellow-orange solution was generated and the bright yellow precipitate that formed was collected,[31] washed with $CH_2Cl_2$ at 273 K, and determined to be $[\mathbf{2_2}][TFAB]_2$ by $^1H$ NMR, IR, elemental analysis, and X-ray diffraction studies. The isolated material exhibited an IR spectrum (KBr) with absorptions at 2083, 2012 $cm^{-1}$ and shoulders at ca. 2092, 2022 $cm^{-1}$ (Supporting Information, Figure SM2), similar to spectra in $C_2H_4Cl_2$ (2071, 2007 $cm^{-1}$, shoulders at ca. 2091, 2034 $cm^{-1}$) and $CH_2Cl_2$ (2076, 2010 $cm^{-1}$, Table 2). Based on the two most intense peaks, a raw average shift[30] for $\nu_{CO}$ of +75 $cm^{-1}$ was calculated in going from **2** IR (2017, 1919 $cm^{-1}$) to $\mathbf{2_2}^{2+}$ (in $CH_2Cl_2$).

**3.1.3. ReCp*(CO)$_3$, 3.** The original anodic peak ($E_{1/2} = 0.91$ V for $\mathbf{3}^{0/+}$) and the cathodic product peaks ($E_{pc} = 0.15$ V for $\mathbf{3_2}^{2+}$ and $E_{pc} = -0.50$ for a secondary product) are shifted negative compared to **1** in response to the electronic effect of permethylation of the Cp ring, the shift of $-0.25$ V in going from $\mathbf{1}^{0/+}$ to $\mathbf{3}^{0/+}$ being exactly as predicted.[32] CV scan rates as high as 5 V $s^{-1}$ did not completely outrun the influence of the dimerization process when concentrations of 1 mM or greater were studied. Digital simulations (Figure 7) gave good fits of the CV curves from 0.2 to 5 V $s^{-1}$, being successfully modeled by a dimerization equilibrium constant of $K_{dim} = 10^5$ $M^{-1}$ and a dimerization rate constant of $8.5 \times 10^3$ $M^{-1}$ $s^{-1}$. These values are within an order of magnitude of those calculated for the dimerization of $\mathbf{1}^+$ (Table 3), showing that the physical parameters of the dimerization process are not greatly affected by permethylation of the Cp ring. In terms of generating stable solutions of the dimer dication $\mathbf{3_2}^{2+}$, bulk anodic electrolyses were somewhat less successful than those used for the Cp and ($C_5H_4NH_2$) analogues. A room-temperature electrolysis of 0.82 mM **2** (1.35 F) gave about a 50% yield of secondary products having cathodic waves at $E_{pc} = -0.50$ and $-0.85$ V. Back-electrolysis at an $E_{appl}$ value negative of both side products regenerated 90% of the starting material **3**. The overall chemical reversibility of these processes suggests that atom-abstraction reactions producing $[ReCp^*(CO)_3X]^+$, X = halide or hydride, may also be responsible for the side reactions in this case. Improved yields of the dimer dication were obtained at lower temperatures: 1.1 F was released for electrolysis of a 1.5 mM solution at 243 K, with only 10% secondary products being observed.

At higher concentrations (5−12 mM) and a temperature of 240 K, anodic electrolyses proceeded smoothly until late in the electrolysis, when pure $[\mathbf{3_2}][TFAB]_2$ precipitated from the solution. An isolated yield of 79% was obtained in the electrolysis of 12 mM **3** at 243 K (see Experimental Section). IR spectra of this solid in nujol had the highest energy $\nu_{CO}$ band at 2062 $cm^{-1}$ and a barely resolved pair at 2018 and 2010 $cm^{-1}$. Unlike the case of $\mathbf{1_2}^{2+}$, only one isomer was observed, presumably the *trans*, in concert with the increased steric requirements of the Cp* ligand. In dichloromethane, the IR bands appeared at 2062 and 2015 $cm^{-1}$, giving a raw average carbonyl shift[30] of +83 $cm^{-1}$ for $\mathbf{3} \rightarrow \mathbf{3_2}^{2+}$, comparable to the values of +97 $cm^{-1}$ and 75 $cm^{-1}$ observed for the Cp and amino-Cp complexes **1** and **2**, respectively. These carbonyl shifts are somewhat smaller than those commonly observed for metal carbonyl compounds differing by one electron. A close analogue of the present compounds is that of the cobalt system recently described,[9] in which the average $\nu_{CO}$ shift was +126 $cm^{-1}$ in going from $CoCp(CO)_2$ to the metal−metal bonded dimer dication $[Co_2Cp_2(CO)_4]^{2+}$. It is useful to keep in mind, however, that whereas the IR spectra of $\mathbf{1_2}^{2+}$ and its analogues contain,

(31) The electrolysis solution appeared to reach supersaturation, in that precipitation of $[\mathbf{2_2}][TFAB]_2$ did not occur until minutes after completion of the electrolysis.

(32) Lu, S.; Stelets, V. V.; Ryan, M. F.; Pietro, W. J.; Lever, A. B. P. *Inorg. Chem.* **1996**, *35*, 1013.

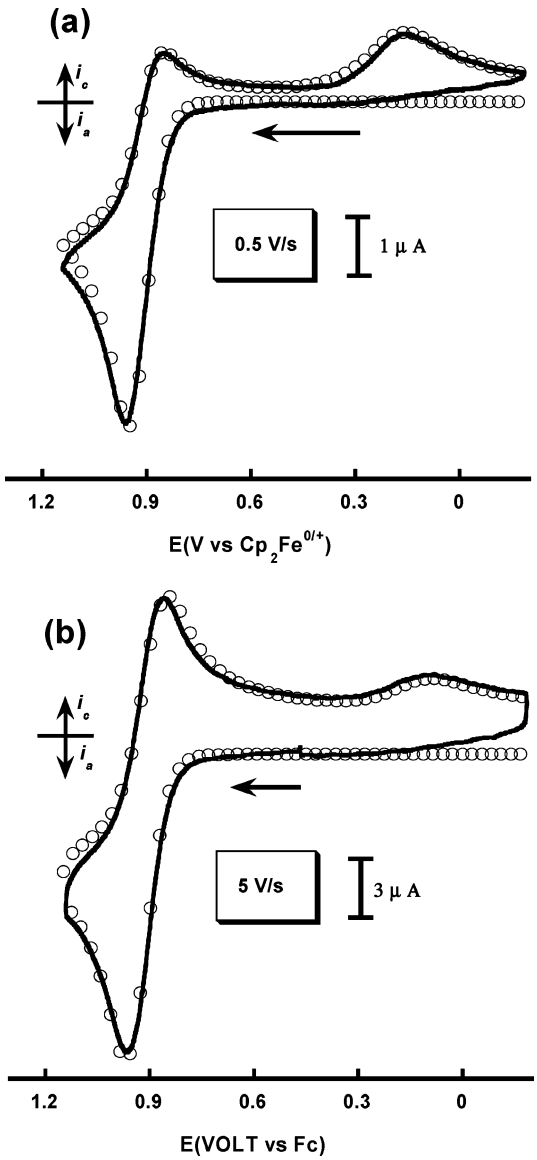


***Figure 7.*** Representative comparisons of experimental (line) and simulated (circles) cyclic voltammograms for 0.86 mM **3** in $CH_2Cl_2$/0.1 M [$NBu_4$][TFAB] at room temperature. Parameters as given in Table 3; also: electrode area 0.0785 $cm^2$; $R_u = 1500\ \Omega$; $C_{dl} = 5 \times 10^{-8}$ F; $D_o$ of $\mathbf{3}_2^{2+}$, $8.6 \times 10^{-6}$ $cm^2\ s^{-1}$; scan rate 0.5 V $s^{-1}$ (top) and 5 V $s^{-1}$ (bottom).

in principle, six fundamental CO bands, only two are resolved, thereby limiting the comparative analysis of the vibrational behavior of the Re complexes.

**3.1.4. X-ray Structure of [$\mathbf{2}_2$][TFAB]$_2$.** The crystalline structure of the amino−dimer dication, shown in Figure 8, confirms the *transoid* orientation of the aminocyclopentadienyl rings and establishes 3.1097(2) Å as the Re−Re bond length. Tables of the measured bond lengths and angles are available as Supporting Information (Tables SM1−SM4), and some structural aspects are discussed below in comparison to the computational results on the parent dimer, $\mathbf{1}_2^{2+}$. One interesting aspect of the amino−Cp structure is the significant out-of-plane bend observed for the cyclopentadienyl ring in $\mathbf{2}_2^{2+}$, for which C(5) is elevated 0.22 Å above the nearly perfect plane of the other four ring carbons. The Re-to-C(5) distance lengthens to 2.554(3) Å as a consequence, over 0.3 Å more than the Re−C(2) and Re−C(3) distances of 2.242(3) and 2.225(3) Å, respectively. The other Re−C distances are 2.324(3) Å [to C(1)] and 2.312(3) Å [to C(4)]. Rationalization of the Cp bending is made more difficult by the fact that the structure of the parent 18-electron complex **2** has not been reported. One cannot rule out the influence of the water molecule (source unknown) which is strongly hydrogen bonded to the amino group: O(4)···HN-(1), 2.87 Å.

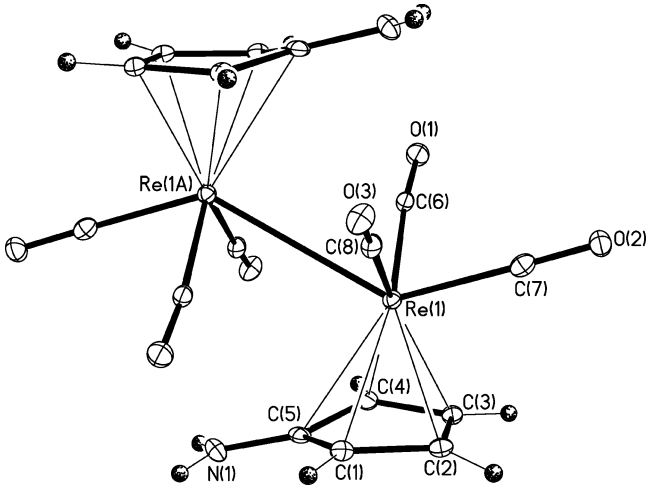


***Figure 8.*** Cationic structure for [$\mathbf{2}_2$][TFAB]$_2$·$2H_2O$ drawn with 30% thermal ellipsoids.

**3.2. Homolytic Cleavage Reactions of [ReCp(CO)$_3$]$^+$.** As mentioned above, an electroactive secondary product ($E_{pc} = -0.16$ V) of roughly 20−30% yield was formed in room-temperature bulk anodic electrolyses of **1** in dichloromethane. It was characterized as the 18-electron chlorocomplex [ReCp-$(CO)_3Cl]^+$, **4**, based on a comparison of its IR and $^1$H NMR properties with an authentic sample of [ReCp$(CO)_3$Cl][TFAB] (the $[SbCl_6]^-$ salt[12d] is insoluble in dichloromethane). To this end, electrolysis of **1** at room temperature gave, in addition to the IR bands noted above for $\mathbf{1}_2^{2+}$, a pair at 2140 and 2085 $cm^{-1}$ (a raw carbonyl shift[30] of +137 $cm^{-1}$) that was identical to those measured separately for **4**. The NMR spectrum of authentic **4**[TFAB] in $CD_2Cl_2$ has its Cp resonance at $\delta = 6.56$ ppm, the precise position of a singlet obtained after bulk electrolysis of **1** in $CD_2Cl_2$/0.02 M [$NBu_4$][TFAB] at 243 K. The chlorocomplex **4** is apparently formed through the homolytic cleavage reaction shown in Scheme 1.

***Scheme 1***

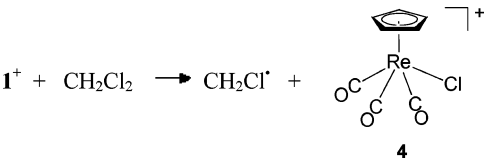


**4**

In order to probe the generality of such homolytic reactions for $\mathbf{1}^+$, CV experiments were performed in which the radical cation was generated in the presence of organic compounds having C−X or C−H bonds that are weaker than that of the C−Cl bond in $CH_2Cl_2$ (bond dissociation energy, BDE, of 81 kcal/mol).[33] Addition of 1 equiv or more of $CH_3I$, $CPh_3Cl$, or 9,10-dihydroanthracene (DHA) resulted, in each case, in complete disappearance of the cathodic wave of the dimer dication $\mathbf{1}_2^{2+}$ and appearance of a new irreversible cathodic feature in the range $E_{pc} = -0.08$ to $-0.20$ V, which we ascribe to the 18-electron products [ReCp$(CO)_3$I]$^+$, [ReCp$(CO)_3$Cl]$^+$,

and $[ReCp(CO)_3H]^+$, respectively. The CV observed upon DHA addition is shown in Supporting Information Figure SM3, wherein the reversible anodic oxidation ($E_{1/2} = 0.83$ V) of the anthracene produced through eq 4 is observed. Bulk anodic electrolysis of **1** in the presence of DHA gave an apparently complete conversion to $[ReCp(CO)_3H]^+$ ($E_{pc} = -0.20$ V assigned to the hydride) and the anthracene radical cation, owing to the fact that anthracene itself undergoes anodic oxidation (eq 5) at the $E_{appl}$ value sufficient to oxidize **1**.

$$2\,[ReCp(CO)_3]^+ + DHA \rightarrow 2\,[ReCp(CO)_3H]^+ + \text{anthracene} \quad (4)$$

$$\text{anthracene} - e^- \rightarrow [\text{anthracene}]^+ \quad (5)$$

Although the production of anthracene might possibly proceed *via* an electron-transfer reaction (DHA to $\mathbf{1}^+$) followed by loss of proton from the $[DHA]^+$ radical cation, it is more likely to be initiated by loss of an H-atom from DHA, which is known to be a facile H-atom donor.[34] Homolytic cleavage reactions appear to be a common reaction pathway of organic hydrides and halides with $\mathbf{1}^+$.

**3.3. Use of $[ReCp(CO)_3]^+$ as a One-Electron Oxidant.** In view of the notably positive potential of $\mathbf{1}^{0/+}$ ($E_{1/2} = 1.16$ V), the feasibility of employing $\mathbf{1}^+$ as a one-electron oxidant for synthetic purposes was probed. The fact that the dimer dication $[\mathbf{1_2}][TFAB]_2$ partially dissociates in solution (eq 2) provides the monomer $\mathbf{1}^+$ for a redox reaction with added substrates, denoted as Red in eq 6. Based on a $K_{dim}$ value between $10^6$ and $10^5$ $M^{-1}$, in a nominally 0.5 mM solution of the pure dimer dication at 298 K, between 4.5% and 14.6% of the ions at equilibrium are the monomer radical $\mathbf{1}^+$.

$$\mathbf{1}^+ + \text{Red} \rightarrow \mathbf{1} + [\text{Red}]^+ \quad (6)$$

The fact that the monomer/dimer equilibrium is coupled to one member of the redox pair $\mathbf{1}/\mathbf{1}^+$ reduces the effective oxidizing power of the radical, since the overall $EC_{dim}$ process of eq 7 has a formal potential, $E^{\circ\prime}$, which is less than the measured $E_{1/2}$ of the $\mathbf{1}^{0/+}$ couple, $E_{1/2}(Re/Re^+)$ (eq 8).

$$2\,\mathbf{1} \rightleftharpoons \mathbf{1_2}^{2+} + 2\,e^- \qquad E^{\circ\prime} \quad (7)$$

$$E^{\circ\prime} = E_{1/2}(Re/Re^+) - 0.029_5 \log K_{dim} \qquad (T = 298\ K) \quad (8)$$

Given a range of $10^5$ to $10^6$ $M^{-1}$ for $K_{dim}$, the oxidizing potential of the Re system is thus reduced from its intrinsic value of $1.16_5$ V for the $\mathbf{1}^{0/+}$ couple to 1.01 to 0.99 V when the oxidant $\mathbf{1}^+$ equilibrates with $\mathbf{1_2}^{2+}$, which occurs rapidly under normal reaction conditions. For synthetic applications of the Re system as an outer-sphere one-electron oxidant, we therefore chose thianthrene ($E_{1/2} = 0.81$ V), $N(C_6H_4Br\text{-}4)_3$ (the reduced form of "magic blue", $E_{1/2} = 0.70$ V) and *bis*(acetylcyclopentadienyl)ferrocene ($E_{1/2} = 0.49$ V) as target substrates for electron-transfer reactions. The radical cations of these systems are among the more popular one-electron oxidizing agents.[15b,35] When a 1 mM $CH_2Cl_2$ solution of either thianthrene or $N(C_6H_4\text{-}Br\text{-}4)_3$ was treated with a nominally 0.5 mM solution of $[\mathbf{1_2}][TFAB]_2$, the solution changed color immediately to the purple of the thianthrene cation radical or the blue of $[N(C_6H_4Br\text{-}4)_3]^+$, respectively. Although the oxidized organic products were not isolated, measurements of the optical spectra of these solutions showed that the reactions were quantitative in the production of the organic radical cation.[36] The bis(acetylcyclopentadienyl) ferrocenium complex $[Fe(C_5H_4COMe)_2]^+$ was, however, isolated as the pure TFAB salt in high yield by this method. See the Experimental Section for details. This general procedure is promising as a way of readily obtaining TFAB salts of oxidized systems having potentials (vs FcH) that are about 0.9 V or less. The oxidizing power of the Re system could be raised by preparing a Re(II) system substituted on the Cp with electron-withdrawing groups or by shutting off the dimerization of $\mathbf{1}^+$, perhaps through surface immobilization of the Re system. These possibilities are under investigation.

**3.4. DFT Calculations.** Calculations[18,19] were performed on the cyclopentadienyl system without symmetry constraints to get the optimized geometries of $ReCp(CO)_3$, $[ReCp(CO)_3]^+$, and the dimer $[Re_2Cp_2(CO)_6]^{2+}$. Two isomers, *cis* and *trans*, were calculated for the dimeric dication, the *trans* form being more stable by 3.7 kcal $mol^{-1}$. We also analyzed the *monocation* radical dimer $[Re_2Cp_2(CO)_6]^+$ ($\mathbf{1_2}^+$). Although it was not detected electrochemically, it is formally analogous to the radical dimer $[Co_2Cp_2(CO)_4]^+$ recently reported as the radical−substrate dimerization product resulting from the oxidation of $CoCp(CO)_2$.[9] Owing to the fact that solvent interactions are likely to be important for half-sandwich metal carbonyl cations,[9] the calculations were carried out using the COSMO model[24] with $CH_2Cl_2$ as the solvent. The differences in geometry (distances and angles) from the gas phase to $CH_2Cl_2$ are negligible, but the energies are significantly corrected. The results described here refer to solvent-based calculations, unless otherwise stated. The optimized geometries (ADF) of **1** and $\mathbf{1}^+$ are shown in Figure 9, with some relevant distances and angles.

The calculated structure of **1** is in good agreement with that determined by X-ray,[37] with three C(O)−Re−C(O) angles very close to 90° and experimental Re−C(O) distances of 1.888, 1.899, and 1.894 Å, compared to the calculated one of 1.917 Å (although no symmetry constraints were considered, the optimized geometry reflects some symmetry, except for $\mathbf{1}^+$, and only part of the numbers is thus given).

The structure of the dimer dication $\mathbf{1_2}^{2+}$ can be compared with the one described above for the amino analogue $\mathbf{2_2}^{2+}$. The calculated Re−Re distance in $\mathbf{1_2}^{2+}$ (3.229 Å) is only slightly longer than the experimental value of 3.0197 Å for $\mathbf{2_2}^{2+}$ (for

(33) Some bond dissociation energies were obtained from the summary in jhu.edu/chem./lectka and were based on values found in the following papers: (a) Goldsmith, C. R.; Jonas, R. T.; Stack, D. P. *J. Am. Chem. Soc.* **2002**, *124*, 83. (b) Blanksby, S. J.; Ellison, G. B. *Acc. Chem. Res.* **2003**, *36*, 255. (c) Senosiain, J. P.; Han, J. H.; Musgrave, C. B.; Golden, D. M. *J. Chem. Soc., Faraday Disc.* **2001**, *119*, 173. (d) McGivern, W. S.; Derecskei-Kovacs, A.; North, S. W. *J. Phys. Chem. A* **2000**, *104*, 436. BDE values: C−I in $CH_3I$, 57.6 kcal/mol; C−H in 9,10-dihydroanthracene, 78 kcal/mol. For C−Cl in $CPh_3Cl$ (50 kcal/mol), see: Köcher, J.; Lehnig, M.; Neumann, W. P. *Organometallics* **1988**, *7*, 1201.

(34) Gupta, R.; MacBeth, C. E.; Young, V. C., Jr.; Borovic, A. S. *J. Am. Chem. Soc.* **2002**, *124*, 1136.

(35) The value for the oxidation of thianthrene was obtained by measurement in our laboratory in $CH_2Cl_2$/0.05 M $[NBu_4][TFAB]$. A somewhat higher value, 0.86 V, was reported earlier for an acetonitrile/$[NBu_4][BF_4]$ medium. See ref 15b and Hammerich, O.; Parker, V. D. *Electrochim. Acta* **1973**, *18*, 537. An apparently quantitative oxidation (based on optical spectroscopy) was also seen when the analyte was $Mn(C_5H_4Me)(CO)_3$, which has a potential of 0.87 V in this medium.

(36) (a) Thianthrene cation: Murata, Y.; Shine, H. *J. Org. Chem.* **1969**, *34*, 3368. (b) Magic blue: O'Connor, A. R.; Nataro, C.; Golen, J. A.; Rheingold, A. L. *J. Organometal. Chem.* **2004**, *689*, 2411.

(37) Fitzpatrick, P. J.; Le Page, Y.; Butler, I. S. *Acta Crystallogr., Sect. B* **1981**, *37*, 1052.

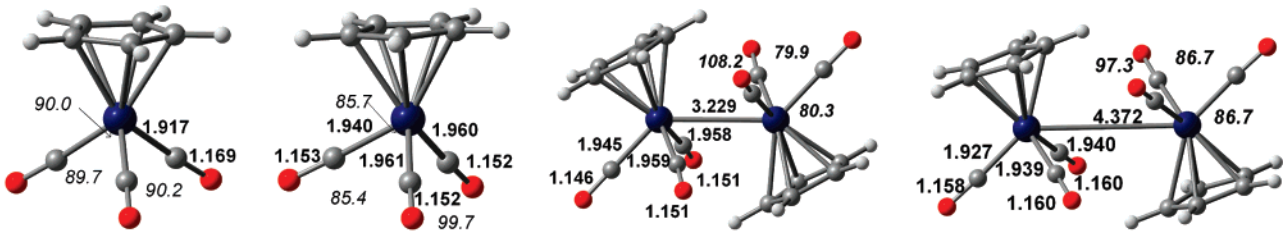


***Figure 9.*** Optimized structures of, left to right, $ReCp(CO)_3$ (**1**), $[ReCp(CO)_3]^+$ ($\mathbf{1}^+$), $[Re_2Cp_2(CO)_6]^{2+}$($\mathbf{1_2}^{2+}$), and $[Re_2Cp_2(CO)_6]^{+\bullet}$ ($\mathbf{1_2}^+$).

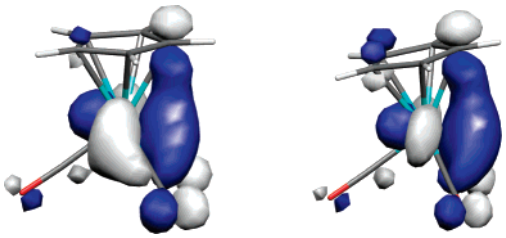

***Figure 10.*** HOMO (left) of $CpRe(CO)_3$ (**1**) and SOMO (right) of $[CpRe(CO)_3]^+$ ($\mathbf{1}^+$).

comparison, the gas-phase calculated Re−Re bond length is 3.271 Å for $\mathbf{1_2}^{2+}$). This may, in fact, reflect the presence of a somewhat weaker Re−Re bond in $\mathbf{1_2}^{2+}$ compared to $\mathbf{2_2}^{2+}$, which would be qualitatively consistent with the fact that the dimer of the amino compound dissociates less in solution. The Re−C(O) bond lengths and angles (Figure 8) show only negligible deviations from the experimental values. Even the asymmetry in the C(O)−Re−C(O) angles is well reproduced, with one wider angle (108.2°) and two narrow ones (~80°). The *trans* form is more stable by 3.7 kcal $mol^{-1}$ and is indeed the isomer found in all experimentally available structures of the family. The dicationic complex $\mathbf{1_2}^{2+}$ was initially identified by IR spectroscopy (Figure 4), and the calculation of frequencies supported this assignment, as the calculated frequencies agree with experimental values for both **1** and $\mathbf{1_2}^{2+}$.

The loss of one electron to form the cation $[CpRe(CO)_3]^+$ ($\mathbf{1}^+$) introduces some asymmetry into the molecule, as well as some lengthening of the Re−C(O) bonds and shortening of the C−O bonds (Figure 9), as a reflection of reduced back-donation from the oxidized metal center. Indeed, the one-electron loss is strongly concentrated on the metal, as can be observed in the representation of the HOMO of **1** (Figure 10), which has also some metal−carbonyl and metal−Cp bonding character. The asymmetry concerns the opening of one C(O)−Re−C(O) angle from ~90° to ~100°, while the other two become narrower (~85°). At the same time, one of the $Cp_{cent}$−Re−C(O) angles, which were ~125° (octahedral angle), drops to 116.9°, and the others widen by ca. 1°−2°. This enables the SOMO of $\mathbf{1}^+$ to change its directionality and become more hybridized away from the metal. The SOMO of the radical cation $\mathbf{1}^+$ thus explains the easy dimerization to form $\mathbf{1_2}^{2+}$and other reactions involving seven-coordinate products or intermediates.

The oxidation potentials were also calculated for the monomeric and the dimeric systems, and the results are shown in Table 4. The experimental oxidation potential (1.16 V) for the pair $\mathbf{1/1}^+$ is very well reproduced by calculations (1.23 V), as long as solvent is considered. In the gas-phase calculation, there is a larger deviation. The other experimental parameter that can also be calculated is the dimerization enthalpy of $\mathbf{1_2}^{2+}$ from two radical cations $\mathbf{1}^+$. The gas-phase value is repulsive (27.8 kcal $mol^{-1}$), since two positively charged species are approaching

***Table 4.*** Calculated (ADF) Absolute ($E_n$) and Relative ($E°_n$ vs FcH) Oxidation Potentials for the Pairs $\mathbf{1/1}^+$ and $\mathbf{1_2}^+/\mathbf{1_2}^{2+}$, Experimental $E°_n$ (Bold), and Dimerization Enthalpies $\Delta H_fn$ (kcal $mol^{-1}$)

| | $E_1$ | $E°_1$ | $\Delta H_f1$ | $\Delta H_f2$ | $E_2$ | $E°_2$ |
|---|---|---|---|---|---|---|
| | $\mathbf{1/1}^+$ | | $(\mathbf{1}+\mathbf{1}^+ \rightarrow \mathbf{1_2}^+)$ | $(\mathbf{1}^+ + \mathbf{1}^+ \rightarrow \mathbf{1_2}^{2+})$ | $\mathbf{1_2}^+/\mathbf{1_2}^{2+}$ | |
| $ReCp(CO)_3$ | 6.21 (8.14)[a] | 1.23 (3.16) **1.16** | −6.4 (−19.7) | −16.6 (27.8) **−6.8**[b] | 5.76 (10.20) | 0.78 (5.22) |

[a] Gas-phase values. [b]Free energy estimated from $K_{eq} = 10^5$ $M^{-1}$.[9]

each other, but the solvent introduces a good correction (−16.6 kcal $mol^{-1}$). From $K_{eq} = 10^5$ $M^{-1}$ we can estimate the experimental value for $\Delta G_{f2}$ as −6.8 kcal $mol^{-1}$. The agreement between the calculated and experimental values is reasonable since we are not considering the entropy effects ($\Delta S < 0$ for an associative process) in the calculation. The inclusion of this term would make $\Delta H_{f2}$ less negative. Also, a better solvent model would probably improve the value.

It can be seen that the formation of the radical dimer $\mathbf{1_2}^+$, from **1** and $\mathbf{1}^+$, is attractive in the absence of solvent, but the enthalpy change for the formation of $\mathbf{1_2}^{2+}$ is more negative than that associated with formation of $\mathbf{1_2}^+$. Even if $\mathbf{1_2}^+$ were formed, it would be promptly oxidized, as its potential is lower that that of **1**. These data are qualitatively different from those observed in the related $CpCo(CO)_2$, which we discussed in detail previously.[9]

## 4. Conclusions

As an important member of the piano-stool family of organometallic compounds, the robust,[2c] IR-active, easily derivatized,[1−3,38] and potentially radioactively labelled[1] $ReCp(CO)_3$ has become widely scrutinized in recent years. However, its electrochemical behavior is only now being seriously probed. The basic molecular orbital model for $ReCp(CO)_3$ describes it as having a quasi-octahedral electronic structure that is reminiscent of ferrocene, at least in terms of its highest occupied orbitals.[39] On that basis, $ReCp(CO)_3$ might be expected to undergo a one-electron oxidation, albeit at a comparatively positive potential owing to its three highly electron-withdrawing carbonyl ligands. The potential of 1.16 V found for $[ReCp(CO)_3]^{0/+}$ is in concert with this expectation. Less predictable, however, were the chemical properties of the 17-electron Re(II) species. Compared to the ferrocenium ion, the metal center in the rhenium system is much more likely to take

(38) (a) Djukic, J-K.; Michon, C.; Heiser, D.; Kyritsakas-Gruber, N.; de Cian, A.; Dötz, K. H.; Pfeffer, M. *Eur. J. Inorg. Chem.* **2004**, 2107 (b) Cesati, R. R.; Katzenellenbogen, J. A. *J. Am. Chem. Soc.* **2001**, *123*, 4093. (c) Minutolo, J. A.; Katzenellenbogen, J. A. *Angew. Chem., Int. Ed.* **1999**, *38*, 1617.
(39) (a) Veiros, L. F. *J. Organometal. Chem.* **1999**, *587*, 221. (b) Albright, T. A.; Burdett, J. K.; Whangbo, M-H. *Orbital Interactions in Chemistry*; John Wiley & Sons: New York, 1985; pp 384−386, 392−394.

on an additional coordinative bond, even in the absence of Cp slippage, owing to its greater (third-row) size.[40] With $\mathbf{1}^+$, coordinative expansion occurs through formation of a Re−Re bond in the dimer dication $\mathbf{1_2}^{2+}$ or, more slowly, by atom-addition reactions, giving 18-electron seven-coordinate species. The DFT results on **1** and $\mathbf{1}^+$ give a clear picture of the orbital makeup that leads to this behavior. Removal of one electron from the mostly metal-based HOMO of **1** significantly lowers the symmetry of the compound, with the resulting rehybridized SOMO of $\mathbf{1}^+$ being directed away from the metal, prompting the high reactivity of the Re(II) center.

The 17-electron monocations of all three Re systems studied, **1**−**3**, were detected by cyclic voltammetry and shown to undergo rapid dimerization giving dications in which the Re−Re bond was unsupported by bridging ligands. The metal−metal bonds of these systems are sufficiently weak to allow partial dissociation in solution, resulting in an equilibrium between monomers and dimers, about 4−14% monomer being calculated for half-millimolar solutions of $\mathbf{1_2}^{2+}$. The dimer dissociation was less prominent for the amino-sustituted compound, perhaps due to the higher metal electron density conveyed by the electron-releasing $NH_2$ group. The dimer dications underwent highly irreversible two-electron reductions, regenerating the corresponding original neutral 18-electron complexes. DFT calculations showed that addition of *one* electron to the dimer dication $\mathbf{1_2}^{2+}$ cleaves the Re−Re bond (calculated Re−Re distance of 4.37 Å in $\mathbf{1_2}^+$, Figure 9), ripping the dimer apart and accounting for the slow heterogeneous charge transfer associated with the electrochemically irreversible cathodic process.

The very positive potentials of the monomer cations make them very strong outer-sphere oxidants which can be readily employed in electron-transfer reactions by taking advantage of the dissociation of the more easily isolated dimer dications. Given the potent and geometrically unencumbered nature of the Re(II) center, the reactions of $\mathbf{1}^+$ with added substrates promise to be of interest, and we are currently pursuing inquiries into possible inner-sphere ET reactions with organic systems.

**Acknowledgment.** We are grateful to the National Science Foundation (CHE 04-11703) for support of this work at the University of Vermont and to FCT and FEDER (POCI/QUIM/58925/2004) for the work in Lisbon. P.J.C. acknowledges FCT for the grant SFRH/BD/10535/2002, and W.E.G. thanks Boulder Scientific Co. for a partial donation of electrolyte anions.

**Supporting Information Available:** Three figures, two showing the IR spectra recorded for isolated $[\mathbf{1_2}][TFAB]_2$ in dichloromethane and of $[\mathbf{2_2}][TFAB]_2$ in KBr, the third showing the CV curve when dihydroanthracene is added to a solution of **1**; four tables giving bond lengths and angles from X-ray analysis of $[Re_2(C_5H_4NH_2)_2(CO)_6][TFAB]_2$. This material is available free of charge via the Internet at http://pubs.acs.org.

JA710513N

(40) Veiros, L. F. *Organometallics* **2000**, *19*, 5549.